Gas Turbine Casing Vibrations under Blade Pressure Excitation

Author:
Forbes, Gareth Llewellyn; Randall, Robert Bond

Publication details:
Proceedings of The 2009 Conference of the Society for Machinery Failure Prevention Technology
pp. 723-733

Event details:
MFPT 2009 Failure Prevention: Implementation, Success Stories and Lessons Learned
Dayton, USA

Publication Date:
2009

DOI:
https://doi.org/10.26190/unsworks/543

GAS TURBINE CASING VIBRATIONS UNDER BLADE PRESSURE EXCITATION

Gareth L. Forbes, Robert B. Randall

School of Mechanical and Manufacturing Engineering, University of New South Wales, Sydney, NSW, 2052, Australia

Abstract: The non-intrusive measurement of the condition of blades within a gas turbine would be a significant aid in the maintenance and continued operation of these engines. Online condition monitoring of the blade health by non-contact measurement methods is the ambition of most techniques. The current dominant method uses proximity probes to measure blade arrival time for subsequent monitoring. It has recently been proposed however, that measurement of the turbine casing vibration response could provide a means of blade condition monitoring, and even give the prospect of providing an estimation of the blade modal parameters. The casing vibration is believed to be excited pre-dominantly by (i) the moving pressure waveform around each blade throughout its motion and (ii) the moments applied by the stationary stator blades. Any changes to the pressure profile around the rotating blades, due to their vibration, will in turn affect these two dominant excitation forces, such that there will be some correlation between the casing response and blade vibrations.
Previous work has introduced an analytical model of a gas turbine casing, and simulated pressure signal, associated with the rotating blades. The effect of individual rotor blade vibrations has been developed in order to understand the complex relationship between these excitation forces. A simplified turbine test rig has been constructed. Various aspects of the previous analytical modelling are presented, and then investigated and verified using results from the experimental program with this simplified test rig.

Keywords: Gas turbines; forced response; casing vibrations; rotor blade vibrations.

Introduction: The internal components of gas turbines operate under the extreme conditions of high stress and temperatures. The main working surfaces inside a turbine engine encountering these conditions are the multiple rotor and stator blade rows. It is of no surprise that analysis of the stress and heat transfer ability of these components has continually been subject to research and development to improve engine design and operating life.

Measurement and modelling of blade vibrations has been developed for two main applications, determination of stress levels induced by the blades' dynamic motion and to quantify blade condition. Analytical [1] and more recently computational [2] models have been developed to determine forced blade motion and stresses taking into account effects such as; wake passing, blade tip vortices, as well as structural and aerodynamic loadings on blades.

The current dominant blade vibration measurement method in the aero-industry [3, 4], during the engine development phase, is blade tip timing (BTT). BTT is achieved through proximity probe measurements obtaining the arrival time of blades at different points around the casing periphery. BTT methods are currently able to satisfactorily measure asynchronous, non-integer multiples of shaft speed, and blade vibrations due to rotating stall, flutter and compressor surge, but require two transducers, perforating the casing, for each blade row. However, no single method is able to fully characterise the vibration parameters of blades in service [5].

An alternative method has been proposed for non-intrusive measurements of blade vibrations by means of external accelerometer measurements on the casing of a gas turbine [6-8]. Investigation into the response of a turbine casing under the influence of operating pressure conditions was first undertaken in [9], with the correlation between measured internal pressure signals and casing vibration measurements shown. Further investigations by the same author have been conducted into the use of unsteady wall pressure signals for blade fault identification in [10] with the extension to CFD simulation of blade faults in [11, 12]. The preceding works have dealt solely with the deterministic periodic forced vibrations. It is thought this is driven by the fact that it is these periodic forces that are usually the most destructive forces within an engine and can cause large deflections and blade stresses. It is however well understood that the operating conditions inside a gas turbine are highly turbulent, due to a wide variety of influences, including but not limited to; ingested turbulence, turbulent boundary layer flow, wake interaction, reversed flow and tip vortex flow. This turbulent flow will result in a more broadband excitation, thus exciting the structural response of the turbine blades over a wide range of frequencies, not just discrete harmonics of shaft speed. It is this broadband excitation which will be exploited in the following analysis.

Measurements of the casing wall pressure and blade vibration signal have been taken from a simplified experimental turbine test rig and are presented within this paper. An analytical simulation of the internal pressure signal is also compared to the experimental measurements. Although the aim of this study is to highlight the ability to obtain blade vibration information from casing vibrations, a comparison between the measured and analytic signal is primarily done on the pressure signal. The results obtained for measured casing vibrations is essentially the same as for the internal pressure signal, with the pressure force passing through the linear time invariant filter of the casing's structural transfer function. Experimental results highlighting this can be found in [13]. However in this case the measurement and interpretation of the pressure signal is less complex than the casing vibration response measurements. Conversely in practice, the ease of making pressure measurements is much less than for accelerometer measurements, since pressure transducers require perforation of the casing and operate in a much harsher environment. Furthermore, the analysis and results within this paper deal predominantly with the effects of the random fluctuations on the mean periodic flow, and it is shown that after separation of the dominant periodic components that the stochastic portion of the pressure contains key information on blade vibrations. It is thought that the second order cyclostationary properties of these stochastic signals should allow separation of effects from the different blade rows (different cyclic frequencies).

Pressure Generation and Blade Response: Flow over the rotor and stator blade aerofoils in a turbine causes high and low pressure forces to act over the blade surfaces. These high and low pressure profiles then interact as the pressure distributions around the rotor blades rotate around, causing fluctuating pressures on the casing surface, as well as interacting with the stationary pressure profiles around the stator blades. Shown schematically in Fig. 1 is the first harmonic of the pressure profile around a set of rotor blades. It can be seen that the pressure on the surface of the casing will therefore vary harmonically with the rate at which blades pass that point, i.e. the blade passing frequency, BPF. Additionally as the rotor blades rotate around the engine they will in turn also be influenced by the varying pressure profile and wakes from the trailing edges of leading stator rows, schematically shown in Fig. 2. The fluctuating forces on the rotor blades will now cause them to vibrate due to the fluctuating pressure, which is driven at the rate which the rotor blades pass through this changing pressure field, i.e. stator passing frequency, SPF.

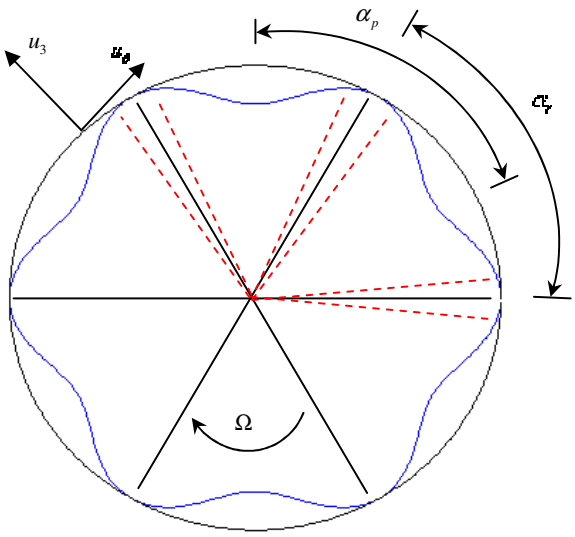

Fig. 1 Cross sectional schematic of turbine casing, blades and pressure profiles. The dashed lines represent blade motion. Note: only 6 blades shown

The pressure acting on rotor blades downstream of a stator blade row has been shown to have, in general, a damped impulse shape [14] (obviously this varies widely and is dependent on the specific turbine). Turbo-machinery flow conditions are however inherently turbulent, with background turbulence intensity levels often reported to be approx. 3-4%, and turbulence within the wake region often five times greater than the background turbulence [15, 16]. It is also noted that the frequency content of turbulence within a gas turbine will be somewhat band-limited; however in the context of this work the turbulence was assumed to be completely broadband.

The forces acting on the rotor blades are therefore modelled as a raised cosine with a period of half the stator blade passing frequency, refer to Fig. 3, and modulated by random fluctuations due to turbulence. The Fourier series expansion of the force on the 'r^{th}' blade can be expressed as:

$$f(t)_r = F_0\left(b(t)+1\right)\left\{\sum_{i=0}^{\infty} A_i \cos\left[i\left(\omega_{spf}t+\gamma_r\right)\right]\right\} \tag{1}$$

$$\gamma_r = \frac{2\pi s(r-1)}{b} - \text{round}\left(\frac{s(r-1)}{b}\right)2\pi \tag{2}$$

where A_i are the Fourier coefficients, ω_{spf} is the stator passing frequency, $b(t)$ is the uniformly distributed random variable with a zero mean and a deviation of $\pm 7.5\%$, with '*s*' the number of stator blades and '*b*' the number of rotor blades.

The rotor blades are modelled as a simple oscillator, i.e. a single degree of freedom spring/mass/damper system, but it will be seen later that the dominant mode in the measurements tends to be the second bending mode. As this would not be known a priori, future analysis should consider modelling with a greater number of modes. Only the solution for the stochastic portion of both the blade motion and pressure force will be obtained in this study for brevity; this is also the portion of the signal that contains the most useful information. Derivation of the solution for the deterministic portion can however be found in [6]. It is also assumed in this analytical model that the motion of adjacent blades does not impact on the response of the blade under consideration.

The solution for the motion of the 'r^{th}' blade can therefore be shown to be:

$$X(f)_r = H(f)_r F(f)_r \tag{3}$$

where capitalization refers to the Fourier transform of the corresponding time signal and $H(f)_r$ is the transfer function of the 'r^{th}' blade being:

$$H(f)_r = \frac{A_r}{\left(\omega_{nb}^2 - \omega^2\right) + 2\zeta_2 j\omega_{nb}\omega} \tag{4}$$

A_r being the gain factor for the 'r^{th}' blade.

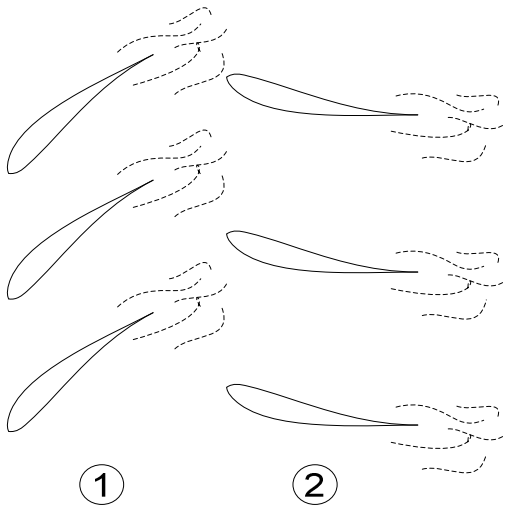

Fig. 2 Wake interaction between stator (1) and rotor (2) blade rows

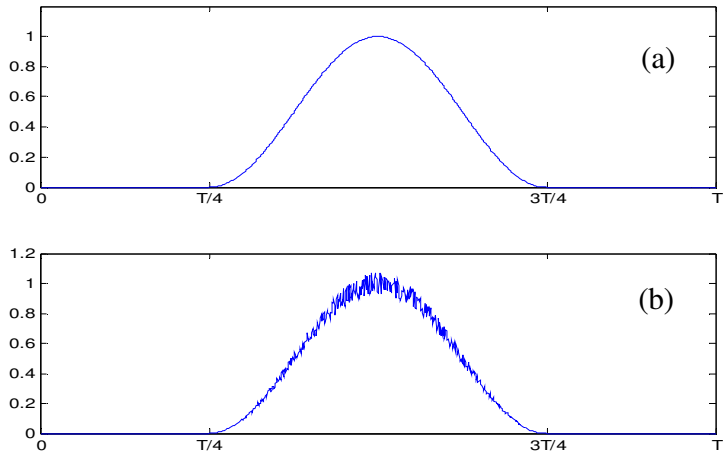

Fig. 3 blade forcing function, purely deterministic (a), with random fluctuations (b)

Pressure on Casing Surface: The pressure generated on the casing surface will be affected by the motion of the blade. This will now cause the pressure around the rotor blades to vary due to the blade motion, with the blade pressure profile following the blade motion as it vibrates about its equilibrium position. The pressure from the 'r^{th}' blade is once again modelled as a raised cosine with half a period of one rotor blade spacing, with the Fourier expansion given as:

$$P_r = \sum_{i=0}^{\infty} A_i . P . e^{ji\left[\theta - \Omega t - x(t)_r - \alpha_r\right]} \tag{5}$$

Note that Eqn. (5) is a rotating sinusoidal pressure with the phase modulated by the blade motion $x(t)$.

Experimental Setup and Measurement: The test rig consists of a 19 flat blade rotor arrangement driven by an electric motor which is currently capable of running at speeds up to 2500rpm. A toroidal ring in front of the bladed arrangement, supplied with high pressure air, provides six jets which act like trailing edge flow from upstream stator blade rows, exciting the rotor blades at multiples of shaft speed. A microphone is flush mounted in the casing in the vertical plane above the rotor blades to measure the pressure inside the casing. One blade was instrumented with an accelerometer placed near the root of the blade, with the signal running through a set slip rings mounted on the input shaft. Measurements were taken with shaft rotational speeds of 1200 and 2000 rpm, and analyzer sampling rate of 65.536 kHz, of which the useful frequency range is 25.6 kHz. Measurement of the casing wall pressure, blade vibration and tacho signal were obtained for a shaft speed of 1200 rpm; however at 2000 rpm, the blade vibration signal could not be captured due to troubles mounting the accelerometer securely at the higher rpm. A tap test was also undertaken on the instrumented blade, while stationary, to obtain the natural frequencies and modes of the blade.

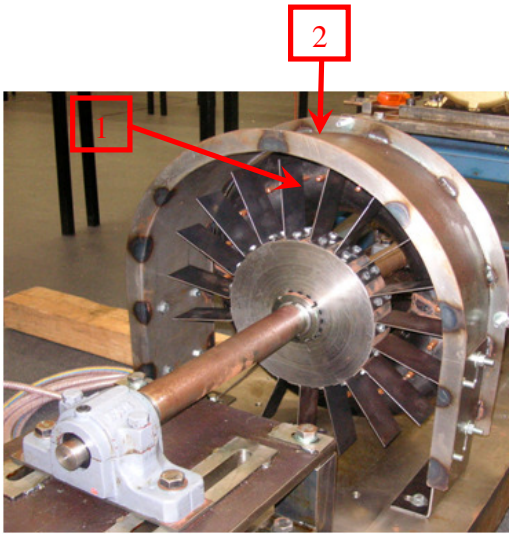

Fig. 4 Experimental test rig. (1) Air jets located on a toroidal ring which is supplied with high pressure air. (2) location of microphone mounting.

The measured signal was re-sampled in the angular domain with an integer number of samples per revolution, triggered by a measured once per-rev tacho signal, normally referred to as order tracking. This has the advantage that the re-sampled signal is compensated for fluctuations due to changes in shaft speed. Phase-locked components are then obtained by time domain synchronous averaging of the order tracked signal, with a period equal to shaft speed, and thus allowing their separation from random components. The power spectrum was then calculated using a hanning weighted, 75% overlapping, Welch-type averaging, resulting in a spectrum with 1 Hz frequency resolution, with 10 effective averages.

Results: The power spectrum, over a limited range of the measured pressure signal is shown in Fig. 5. The residual signal is overlaid on the synchronously averaged discrete signal. The discrete signals can be seen to be made up of multiple discrete peaks at harmonics of shaft speed. The residual signal in Fig. 5 can be seen to be relatively flat with sets of peaks spaced at multiples of shaft speed, the zoomed spectrum in Fig. 6 shows this more clearly.

Table 1 Blade natural frequencies

Mode	Stationary	1200 rpm
1st bending	116.3 Hz	118.8 Hz
1st torsion	515 Hz	522.5 Hz
2nd bending	720 Hz	728.8 Hz

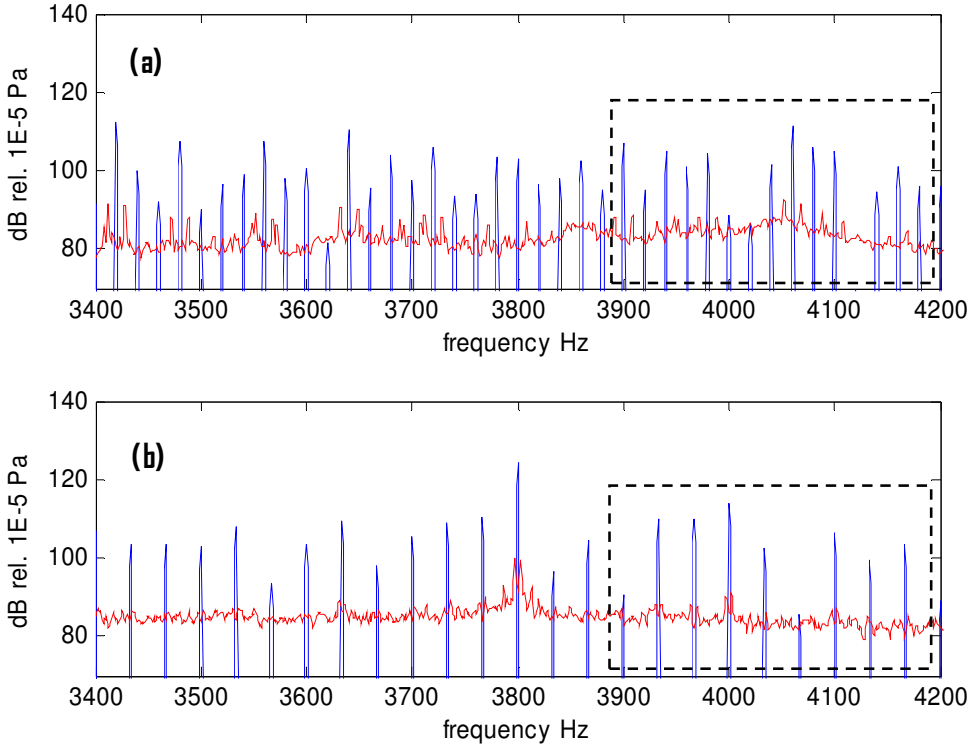

Fig. 5 PSD of measured pressure signal, separated discrete and residual signal overlaid on each other. (a) 1200 rpm (b) 2000 rpm. Zoomed section indicated.

The zoomed spectrum shown in Fig. 6 (a), highlights the narrow band peaks centred around multiples of shaft speed. Multiples of shaft speed are shown by the solid vertical lines; the other vertical dashed lines show the corresponding multiples of shaft speed ± the second bending mode natural frequency. The same harmonic series is shown in Fig. 6 (b) with a second bending mode natural frequency estimated to be 736 Hz. This corresponds well with the expected increase in natural frequency which would result from centrifugal stiffening, as seen in the increase in natural frequencies from stationary measurements and those at 1200 rpm, *Table 1*. Analytical results are also shown, Fig. 6 (c), for the simulated pressure signal, for the same operating conditions as the experimental test rig; i.e. 19 rotor blades, 6 stator blades, and 1200 rpm shaft speed, and blade natural frequency of 728.8 Hz. Within the frequency range shown only the harmonics at multiples of shaft speed + second bending mode natural frequency are visible, which is predominantly the case also for the measured signal at 1200 rpm. Previous results, presented in [13], for 2000 rpm shaft speed, assumed that the first bending mode would be dominant in the response, but this seemed to indicate that the blade natural frequencies were spaced around half order shaft harmonics. However, as is seen, the second bending mode seems to be the dominant displacement visible in the measured signals, this being confirmed by measurement of the actual blade response.

The measured blade displacement, at 1200 rpm, is seen in Fig. 7, with the first and second bending and first torsional mode indicated in Fig. 7 (a), also shown are narrow

band peaks at 2 and 4 x shaft speed. The zoomed section, shown in Fig. 7 (b), shows a harmonic series of peaks spaced at shaft speed – second bending and first torsional mode. The appearance of these peaks, show that adjacent blade motion influences the forcing of other blades. In the current analytical modeling this is not assumed, which would mean only the blade's structural response should be seen in the measured blade displacement, cf. Eqn. (3).

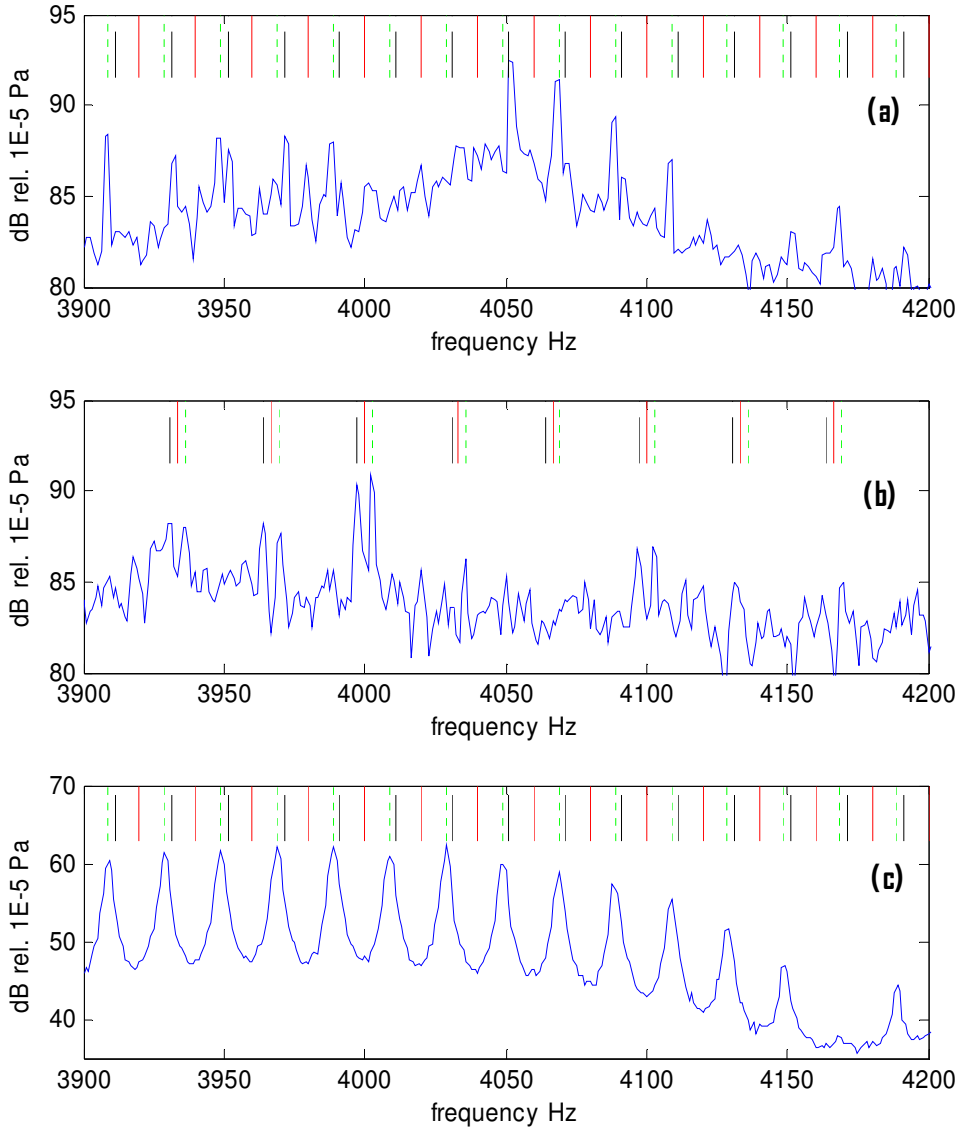

Fig. 6 Zoomed spectrum of the measured residual pressure signal. Vertical —— line at shaft speed spacing, vertical ---- line at shaft speed – second bending mode natural frequency, vertical ..... line at shaft speed + second bending mode natural frequency. (a) 1200 rpm (b) 2000 rpm (c) analytical 1200 rpm

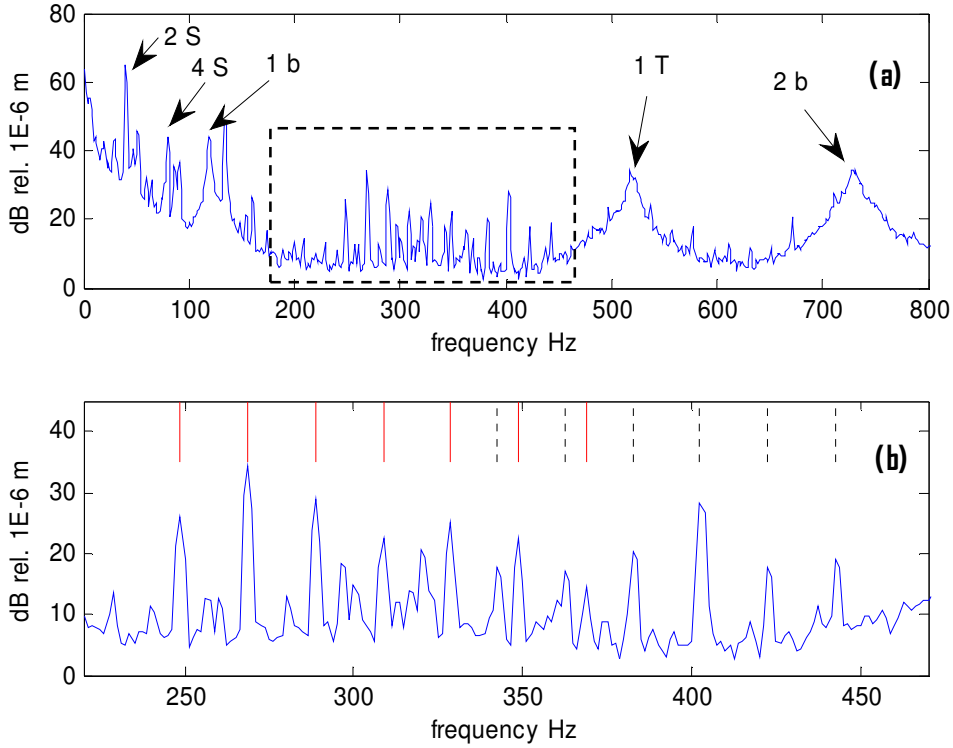

Fig. 7 (a) Measured spectrum of blade displacement at 1200rpm. Indicated: 2, 4 x shaft speed; 2 S, 4S. 1st and 2nd bending modes; 1 b, 2 b. 1st torsional mode; 1 T. (b) Zoomed section as indicated in (a). Vertical —— line at multiples of shaft speed – 2 b, vertical ..... line at shaft speed – 1 T.

Conclusions: Measured casing wall pressure, and blade displacement have been presented along with the analytical formulations of the internal pressure signal for a simplified turbine test rig. Results for the simulated pressure signal shown here and in previous work have been shown to contain the same signal features as those which have been measured, namely; discrete peaks at multiples of shaft speed and narrow band peaks at multiples of shaft speed ± blade natural frequency. Importantly, this gives the ability to obtain a direct measure of a blade's natural frequency at a single running speed, which was previously not possible using the forced vibration at a harmonic of shaft speed. In contrast to previous studies, [13], the residual signal has been shown to be dominated by the second bending mode (on this test rig), which points to the need for future modelling to include more than one mode in the blade dynamic model. The influence of adjacent blade motions on each other has also been shown to occur and inclusion of this effect could improve further modelling. It is thought that motion of actual turbine blades is much more dominated by the first bending mode, than was found to be the case for this test rig. Moreover, this first bending mode is likely to be of the same order as the shaft speed in an actual turbine, rather than an order of magnitude less as with this test rig.

Acknowledgements: Grateful acknowledgment is made for the financial assistance given by the Australian Defence Science and Technology Organisation, through the Centre of Expertise in Helicopter Structures and Diagnostics at UNSW.

References:

1. Majjigi, R.K. and P.R. Gliebe, *Development of rotor wake/vortex model*, in *NASA-CR-174849*. 1984, NASA contract NAS3-23681.
2. Chiang, H.-W.D. and R.E. Kielb, *Analysis system for blade forced response.* Journal of Turbomachinery, Transactions of the ASME, 1993. **115**(4): p. 762-770.
3. Zielinski, M. and G. Ziller, *Noncontact Blade Vibration Measurement System for Aero Engine Application.* American Institute of Aeronautics and Astronautics, 2005(ISABE).
4. Heath, S., *A New Technique for Identifying Synchronous Resonances Using Tip-Timing*. Journal of Engineering for Gas Turbines and Power, 2000. **122**(2): p. 219-225.
5. Heath, S., et al. *Turbomachinery blade tip measurement techniques*. in *Advanced Non-Intrusive Instrumentation for Propulsion Engines*. 1997. Brussels, Belgium.
6. Forbes, G.L. and R.B. Randall. *Simulated Gas Turbine Casing Response to Rotor Blade Pressure Excitation*. in *5th Australasian Congress on Applied Mechanics*. 2007. Brisbane, Australia.
7. Forbes, G.L. and R.B. Randall. *Separation of excitation forces from simulated gas turbine casing response measurements*. in *EURODYN 2008*. 2008. Southampton, UK.
8. Forbes, G.L. and R.B. Randall. *Detection of a Blade Fault from Simulated Gas Turbine Casing Response Measurements*. in *4th European Workshop on Structural Health Monitoring* 2008. Krakow, Poland.
9. Mathioudakis, K., E. Loukis, and K.D. Papailiou. *Casing vibration and gas turbine operating conditions*. 1989. Toronto, Ont, Can: Publ by American Soc of Mechanical Engineers (ASME), New York, NY, USA.
10. Mathioudakis, K., et al., *Fast response wall pressure measurement as a means of gas turbine blade fault identification.* Journal of Engineering for Gas Turbines and Power, Transactions of the ASME, 1991. **113**(2): p. 269-275.
11. Dedoussis, V., K. Mathioudakis, and K.D. Papiliou. *Numerical simulation of blade fault signatures from unsteady wall pressure signals*. 1994. Hague, Neth: Publ by ASME, New York, NY, USA.
12. Stamatis, A., N. Aretakis, and K. Mathioudakis. *Blade fault recognition based on signal processing and adaptive fluid dynamic modelling*. 1997. Orlando, FL, USA: ASME, New York, NY, USA.
13. Forbes, G.L. and R.B. Randall. *Gas Turbine Casing Response to Blade Vibrations: Analytical and Experimental results*. in *AIAC-13, Sixth DSTO International Conference on Health & Usage Monitoring*. 2009. Melbourne, Australia: DSTO.

14. Mailach, R., L. Muller, and K. Vogeler, *Rotor-stator interactions in a four-stage low-speed axial compressor - Part II: Unsteady aerodynamic forces of rotor and stator blades.* Journal of Turbomachinery, 2004. **126**(4): p. 519-526.
15. Henderson, A.D., G.J. Walker, and J.D. Hughes, *The influence of turbulence on wake dispersion and blade row interaction in an axial compressor.* Journal of Turbomachinery, 2006. **128**(1): p. 150-157.
16. Dullenkopf, K. and R.E. Mayle, *Effects of incident turbulence and moving wakes on laminar heat transfer in gas turbines.* Journal of Turbomachinery, Transactions of the ASME, 1994. **116**(1): p. 23-28.